Electronic Supporting Information

Dual-infinite coordination polymers-engineered nanomedicines for dual-ions interference-mediated oxidative stress-dependent tumor suppression

Junlie Yao,[ab] Jie Xing,[a] Fang Zheng,[a] Zihou Li,[a] Shunxiang Li,[a] Xiawei Xu,[a] Devrim Unay,[d] Young Min Song,[e] Fang Yang*[ac] and Aiguo Wu*[ac]

[a] Cixi Institute of Biomedical Engineering, International Cooperation Base of Biomedical Materials Technology and Application, Chinese Academy of Sciences (CAS) Key Laboratory of Magnetic Materials and Devices, Zhejiang Engineering Research Center for Biomedical Materials, Ningbo Institute of Materials Technology and Engineering, CAS, Ningbo 315201, China

[b] University of Chinese Academy of Sciences, No. 1 Yanqihu East Road, Huairou District, Beijing, 101408, China

[c] Advanced Energy Science and Technology Guangdong Laboratory, Huizhou 516000, P.R. China

[d] Electrical and Electronic Engineering Izmir Democracy University, Karabaglar 35140, Turkey

[e] School of Electrical Engineering and Computer Science, Gwangju Institute of Science and Technology, Gwangju 61005, Republic of Korea

*Corresponding author, E-mail: yangf@nimte.ac.cn, aiguo@nimte.ac.cn

Experimental Methods

Materials: 1,1'-Ferrocenedicarboxylic acid was purchased from Sinopharm Chemical Reagent Co.,Ltd. (Shang hai, China). Calcium chloride anhydrous ($CaCl_2$), Tannic acid (TA), Methanol, Polyvinyl pyrrolidone (PVP, Mw = 40,000), 1,10-Phenanthroline,1,2-Distearoyl-sn-glycero-3-phosphoethanolamine-N-[methoxy(polyethyleneglycol)] (DSPE-PEG, Mw = 2000), 3,3',5,5'-Tetramethylbenzidine (TMB), Potassium ferricyanide, Alizarin red, and 2,7-Dichlorofluorescin diacetate (DCFH-DA) were purchased from Aladdin Reagent, Ltd. (Shanghai, China). All other chemical agents are of analytical grade and used as received.

Synthesis of Fc NPs: 1,1'-Ferrocenedicarboxylic acid (20 mg) and Methanol (30 mL) were evenly mixed under ultrasound (50 W, 10 min), and the as-mixed system was exposed to the light-emitting diode (LED) light (0.02 W, 90 min) in the stirred state to prepare Fc ICPs. The centrifugally collected Fc ICPs were dispersed by deionized water (10 mL) dissolving DSPE-PEG 2000 (5 mg), and then processed by ultrasound (150 W, 20 min) to prepare Fc NPs. The centrifugally collected Fc NPs were dispersed in deionized water (5 mL).

Synthesis of Fc@Ca-TA NPs: Fc NPs solution (1 mL), $CaCl_2$ (250 μg), and TA (125 μg) were evenly mixed under ultrasound (50 W, 10 min). Then, Tris-HCl buffer solution at pH 8.5 (500 μL) was added into the as-mixed system under ultrasound (50 W, 5 min). Next, PVP 40000 (2 mg) was added into the as-mixed system under ultrasound (100 W, 10 min) to prepare Fc@Ca-TA NPs. The centrifugally collected Fc@Ca-TA NPs were stored at 4 °C.

Evaluation of degradation performance: Fc@Ca-TA NPs (Fe: 50 μg mL^{-1}) were dispersed in PBS buffer solutions at pH 7.4 or 5.5. Then, the centrifugally collected supernatants were used for inductively coupled plasma optical emission spectrometry (ICP-OES; SPECTRO, Germany) detection to obtain Fe/Ca release. Furthermore, Fe^{2+} was determined by the 1,10-Phenanthroline colorimetric method.

Evaluation of ·OH generation performance: Fc@Ca-TA NPs (Fe: 10 μg mL^{-1}) were dispersed in PBS buffer solutions at pH 7.4 or 5.5 for 24 h. Then, the centrifugally collected supernatants were mixed with H_2O_2 (1 mM) and TMB (1 mM) for ·OH colorimetric detection. Furthermore, electron spin resonance (ESR) was used for ·OH direct detection using 5,5-Dimethyl-1-pyrroline N-oxide (DMPO).

Evaluation of MR imaging performance: Fc@Ca-TA NPs (Fe: 0-25 μg mL^{-1}) were dispersed in PBS buffer solutions at pH 7.4 or 5.5 for 24 h, and then used for imaging capability and relaxometry detection using 3.0 T magnetic property measurement system (Quantum Design, USA).

Preliminary bioinformatics analysis: Gene sets about calcium homeostasis (GOBP_CALCIUM_ION_TRANSPORT, GOBP_RESPONSE_TO_CALCIUM_ION, GOBP_REGULATION_OF_CYTOSOLIC_CALCIUM_ION_CONCENTRATION, GOBP_IRON_ION_TRANSPORT, KEGG_CALCIUM_SIGNALING_PATHWAY) and iron homeostasis (GOBP_CELLULAR_IRON_ION_HOMEOSTASIS, GOBP_IRON_ION_HOMEOSTASIS, HP_ABNORMALITY_OF_IRON_HOMEOSTASIS, GOBP_IRON_ION_TRANSPORT, GOBP_RESPONSE_TO_IRON_ION, REACTOME_IRON_UPTAKE_AND_TRANSPORT) were obtained from MSigDB online database (http://www.gsea-msigdb.org/gsea/login.jsp).

Cell lines and animals: MDA-MB-231/MCF-7/3T3/L929 cells were purchased from the Cell Bank of the Chinese Academy of Sciences (Shanghai, China), while Female BALB/c mice were purchased from Nanjing Cavins Biotechnology Co., Ltd. (Nanjing, China). All animal experiments were approved by the Science and Technology Department of Zhejiang Province [SYXK (Zhe) 2019-0005].

Evaluation of cytotoxicity: MDA-MB-231/MCF-7/3T3 cells were cultured with Dulbecco's modified Eagle's medium (DMEM) dissolving Fc@Ca-TA NPs (Fe: 0-100 μg mL^{-1}) for 24 h, and then used for Cell Counting Kit-8 (CCK8) detection. In

addition, the cellular uptake performance was further investigated using FITC-labeled Fc@Ca-TA NPs (Fe: 50 μg mL^{-1}) via flow cytometric analysis.

Observation of intracellular calcium generation: MDA-MB-231 cells were cultured with DMEM dissolving Fc@Ca-TA NPs (Fe: 0-100 μg mL^{-1}) for 12 h. Then, MDA-MB-231 cells were stained with Fluo-4 AM fluorescent probe (Beyotime Biotechnology Co., Ltd., Shanghai, China) and observed via Leica confocal laser scanning microscope (CLSM; TCS SP8, Germany).

Observation of intracellular oxidative stress: MDA-MB-231 cells were cultured with DMEM dissolving Fc@Ca-TA NPs (Fe: 100 μg mL^{-1}) for 12 h. Then, MDA-MB-231 cells were stained with DCFH-DA for ROS generation detection; mitochondrial membrane potential (MMP) were explored using a JC-1 staining kit (Beyotime) and an Rho 123 staining kit (BestBio Biotech Co., Ltd., Shanghai, China); glutathione (GSH), superoxide dismutase (SOD), adenosine triphosphate (ATP) levels were explored using a GSH assay kit (Solarbio Science & Technology Co., Ltd., Beijing, China), a SOD assay kit (Sangon Biotech Co., Ltd., Shanghai, China), and a ATP assay kit (Beyotime); pretreated (e.g. dehydration, embedding, and sectioning) cells were observed via Hitachi bio-transmission electron microscopy (Bio-TEM; HT7800, Japan).

Exploration of cell death mode: MDA-MB-231 cells were cultured with DMEM dissolving Fc@Ca-TA NPs (Fe: 100 μg mL^{-1}) for 24 h. Then, pretreated (e.g. dehydration, embedding, and sectioning) cells were observed via scanning electron microscope (SEM; SU8230; Japan). Furthermore, Caspase-3, Caspase-8, and Caspase-9 activities as well as apoptosis rate were detected using Caspase and annexin V-FITC/PI apoptosis assay kits (Beyotime).

Biosafety analysis: Experimental mice were intravenously injected with Fc@Ca-TA NPs (Fe: 8 mg mL^{-1}, 100 μL). After 14 days, the blood of sacrificed mice was used for biochemical analysis, and their stained organs were used for histopathological diagnosis.

Evaluation of *in vivo* tumor elimination: MDA-MB-231 tumor-bearing mice were randomly divided into a control group and two treatment groups once the tumor volume reached approximately 50 mm^3. Control group: mice were intravenously injected with saline on day 0, 2 and 4; Treatment groups: mice were intravenously or intratumorally injected with Fc@Ca-TA NPs (Fe: 4 mg mL^{-1}, 50 μL) on day 0, 2 and 4.

Evaluation of *in vivo* MR imaging: After intratumorally or intravenously injecting Fc@Ca-TA NPs (Fe: 4 mg mL^{-1}, 50 μL), MDA-MB-231 tumor-bearing mice were used to analyze the MR imaging property of Fc@Ca-TA NPs using 0.5T MesoMR23-060H-1 (Niumag, China).

Statistical analysis: All experimental data were expressed as the mean ± SD. In addition, the significant differences were acquired via GraphPad Prism 7 software (*** means $P < 0.001$, ** means $P < 0.01$, and * means $P < 0.05$).

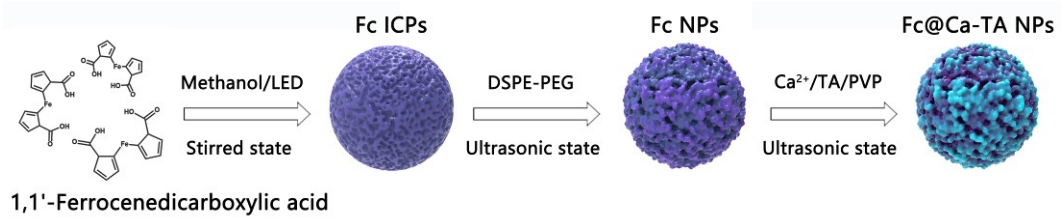

Fig. S1. Illustration of the preparation of Fc@Ca-TA NPs.

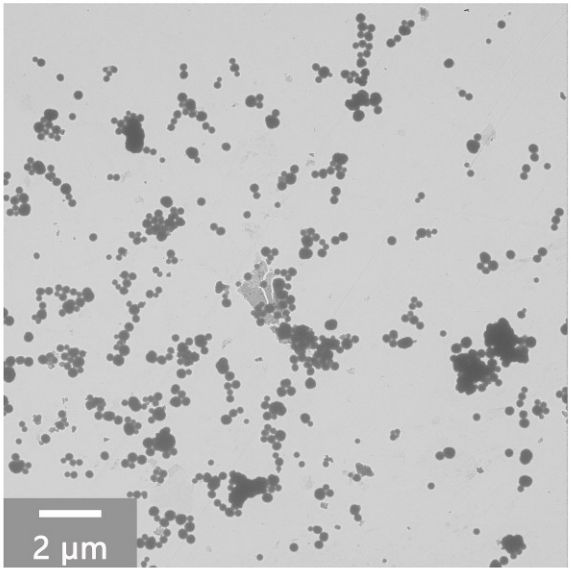

Fig. S2. Low-magnification TEM image of Fc NPs.

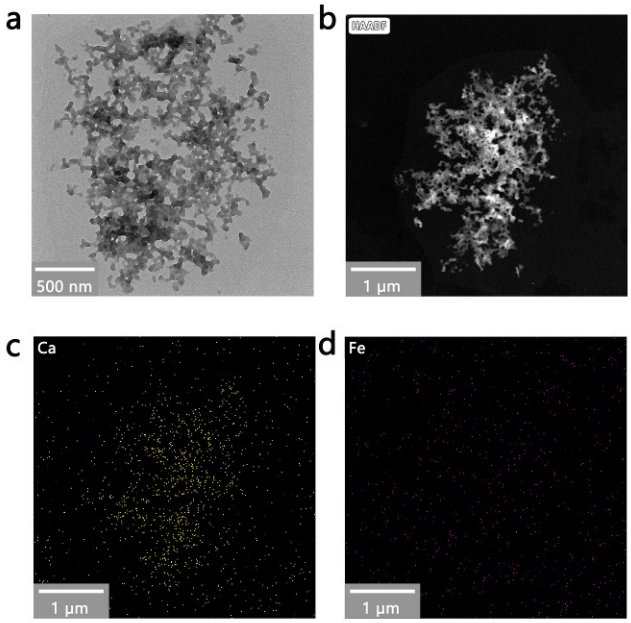

Fig. S3. (a) TEM image of Fc@Ca-TA particles without DSPE-PEG. (b-d) EDS spectrum of Fc@Ca-TA particles without DSPE-PEG. Without the addition of DSPE-PEG, the final product had irregular morphology and relatively high calcium content rather than iron.

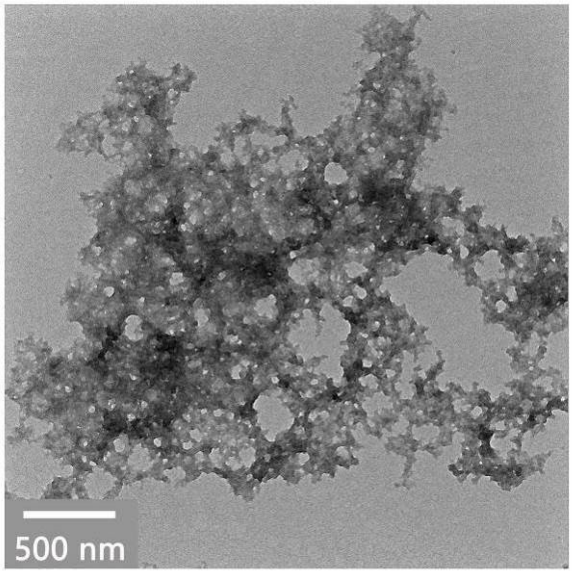

Fig. S4. TEM image of Ca-TA@PVP particles. Without Fc NPs as substrates, Ca^{2+} ions can still form ICPs with tannic acid. Nevertheless, Ca-TA@PVP particles had an irregular shape with non-nanoscale size distribution.

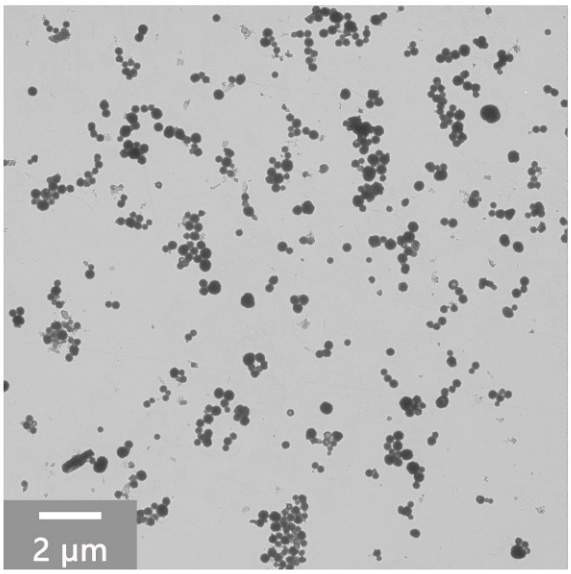

Fig. S5. Low-magnification TEM image of Fc@Ca-TA NPs.

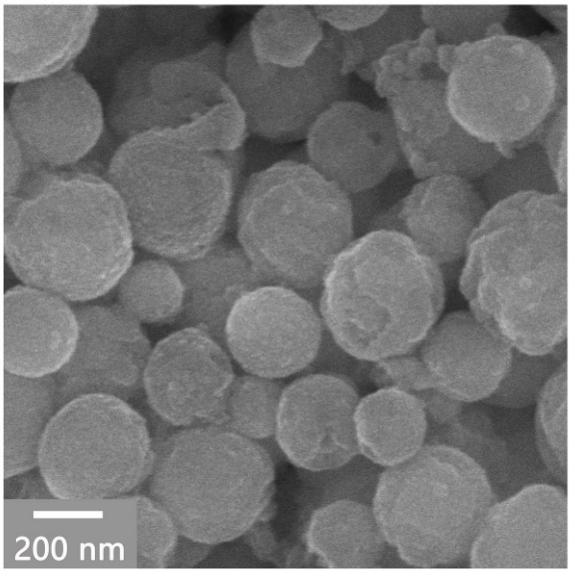

Fig. S6. SEM image of Fc@Ca-TA NPs.

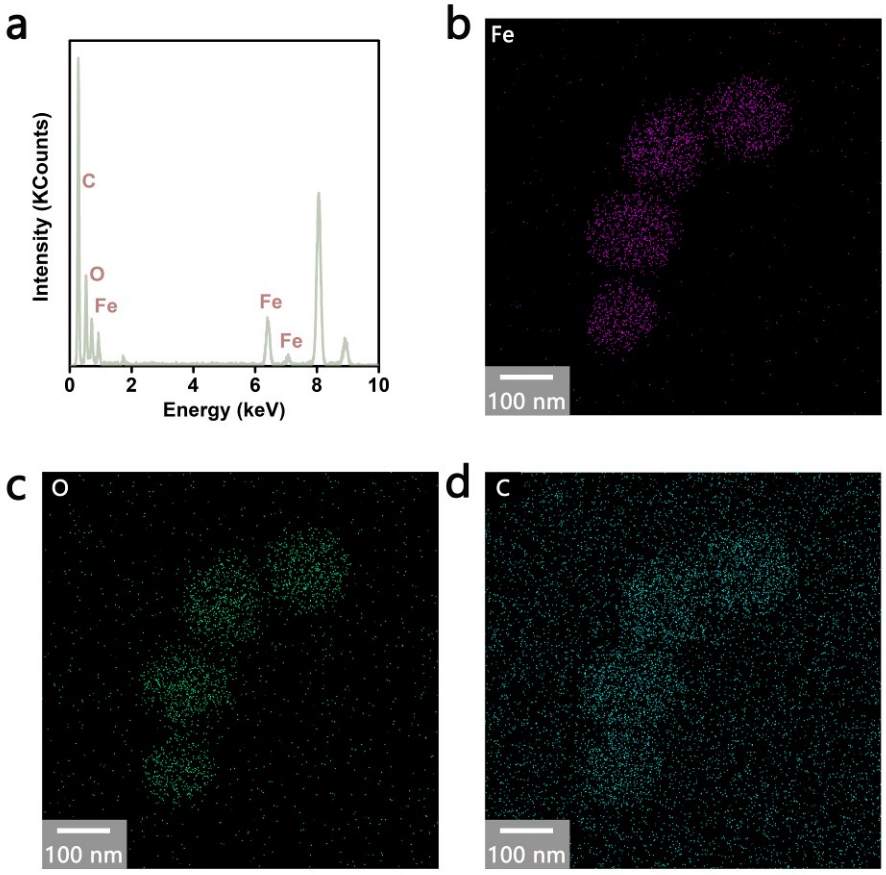

Fig. S7. (a) EDS spectrum of Fc NPs. (b-d) Elemental mapping of Fc NPs. There was no Ca^{2+} in the Fc NPs.

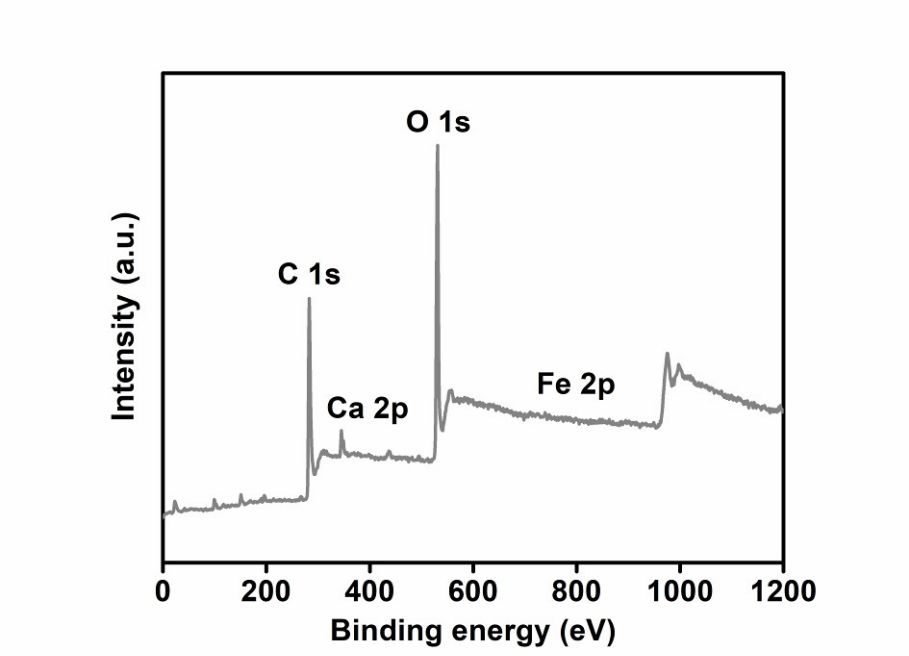

Fig. S8. XPS survey spectrum of Fc@Ca-TA NPs.

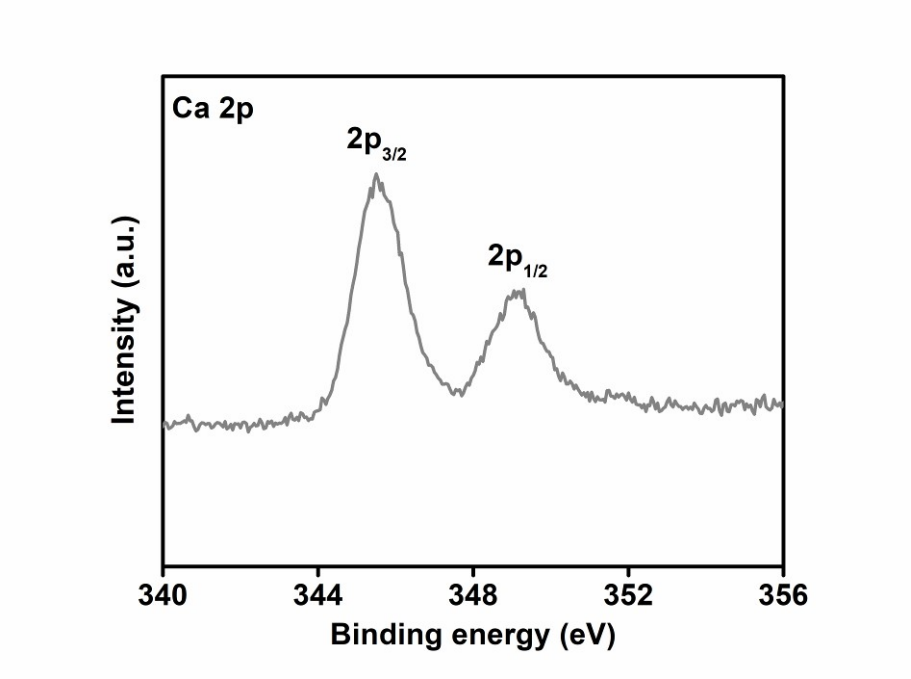

Fig. S9. High-resolution Ca 2p spectrum of Fc@Ca-TA NPs.

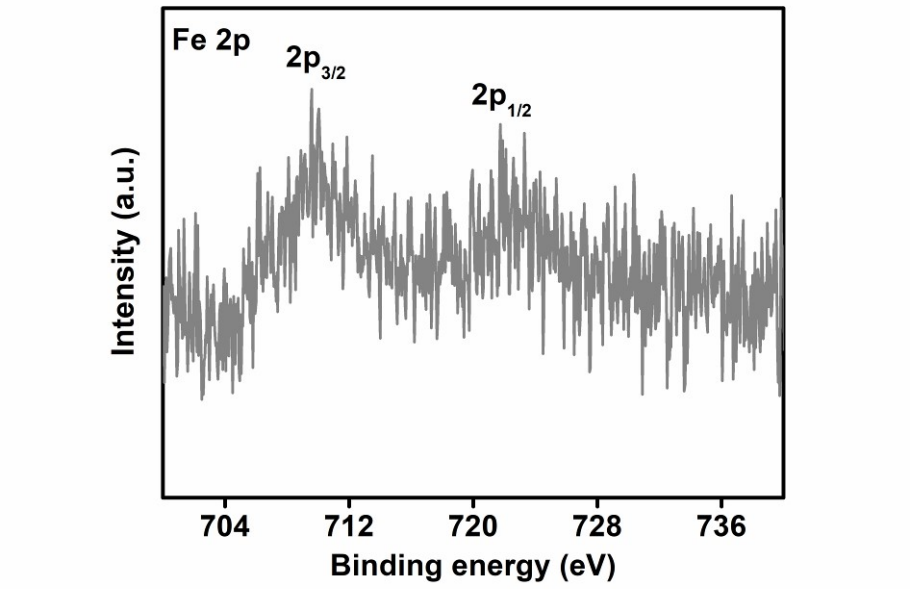

Fig. S10. High-resolution Fe 2p spectrum of Fc@Ca-TA NPs.

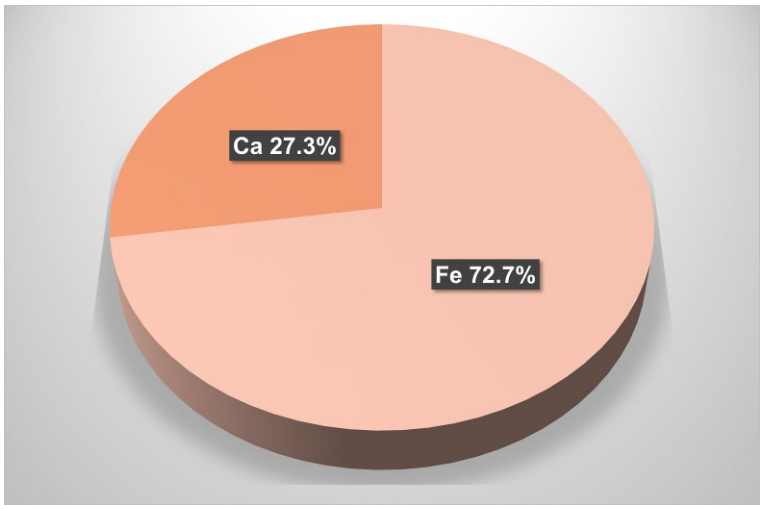

Fig. S11. Metal content ratio in the Fc@Ca-TA NPs.

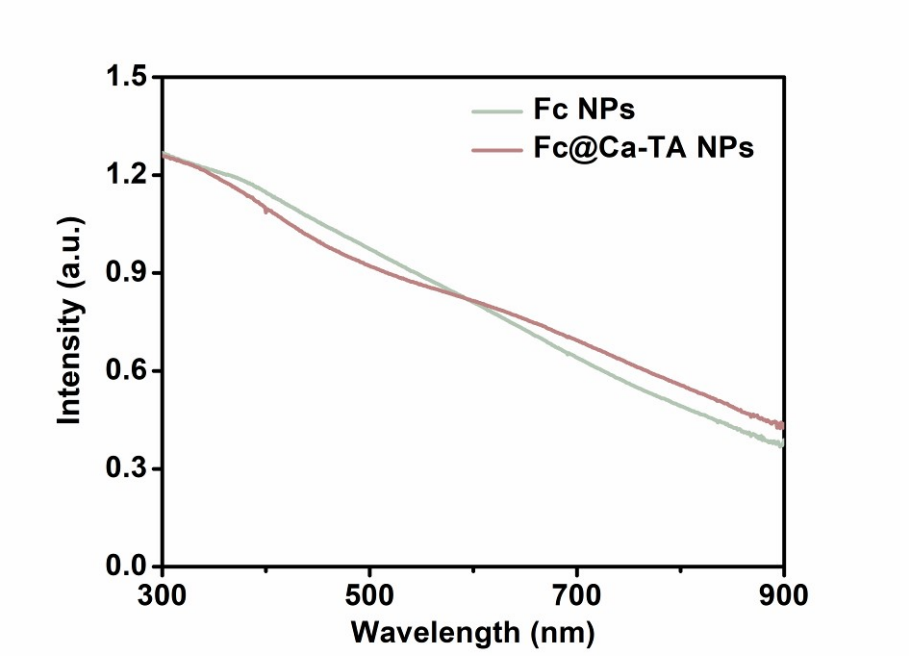

Fig. S12. UV−vis absorption spectra of Fc NPs and Fc@Ca-TA NPs. Neither Fc NPs nor Fc@Ca-TA NPs had a significant absorption peak.

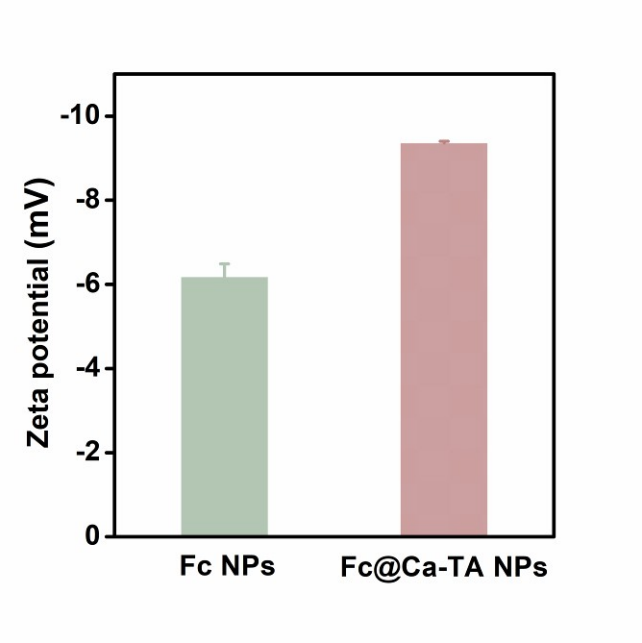

Fig. S13. Zeta potentials of water dispersible Fc NPs and Fc@Ca-TA NPs. Data are presented as the mean ± SD (n = 3). Both Fc NPs and Fc@Ca-TA NPs were negatively charged in deionized water.

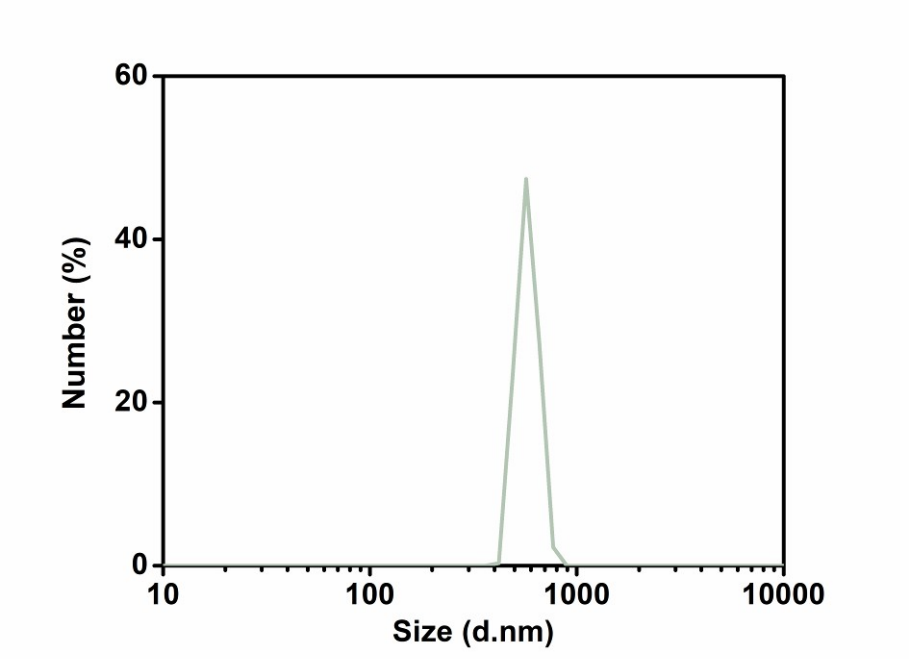

Fig. S14. DLS curves of Fc@Ca-TA NPs (after acid degradation). After acid degradation, the morphology of Fc@Ca-TA NPs changed from spherical to irregular lamellar, accompanied by the increase of particle size.

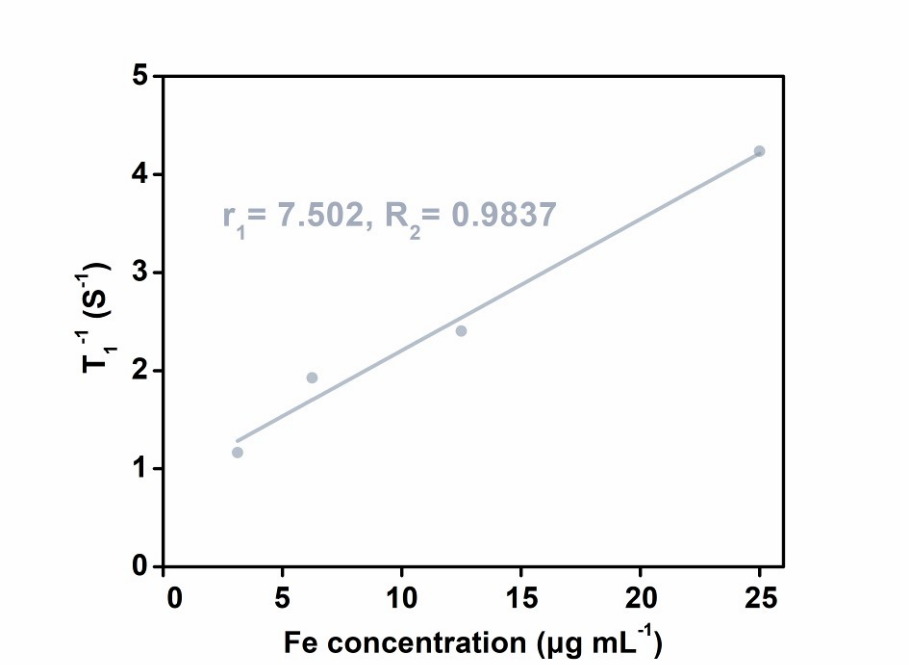

Fig. S15. MR longitudinal relaxation curve of Fc@Ca-TA NPs (at pH 5.5).

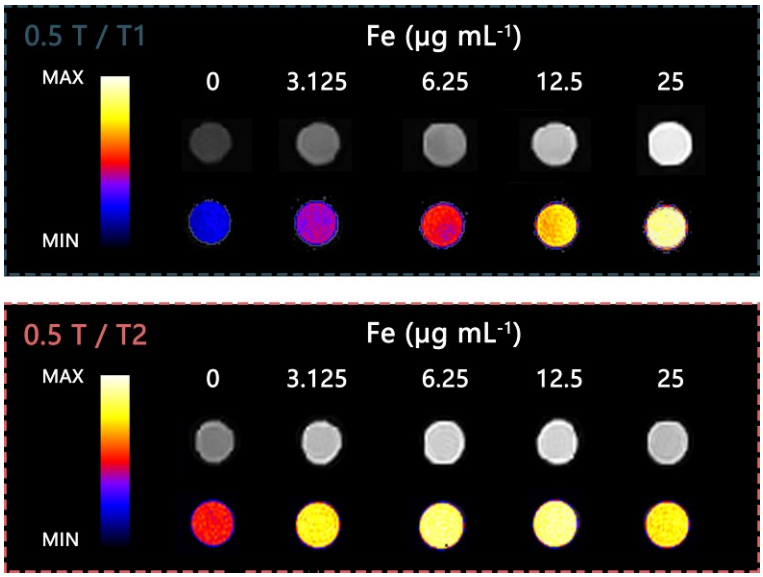

Fig. S16. T_1-weighted and T_2-weighted MR images of Fc@Ca-TA NPs (after acid degradation).

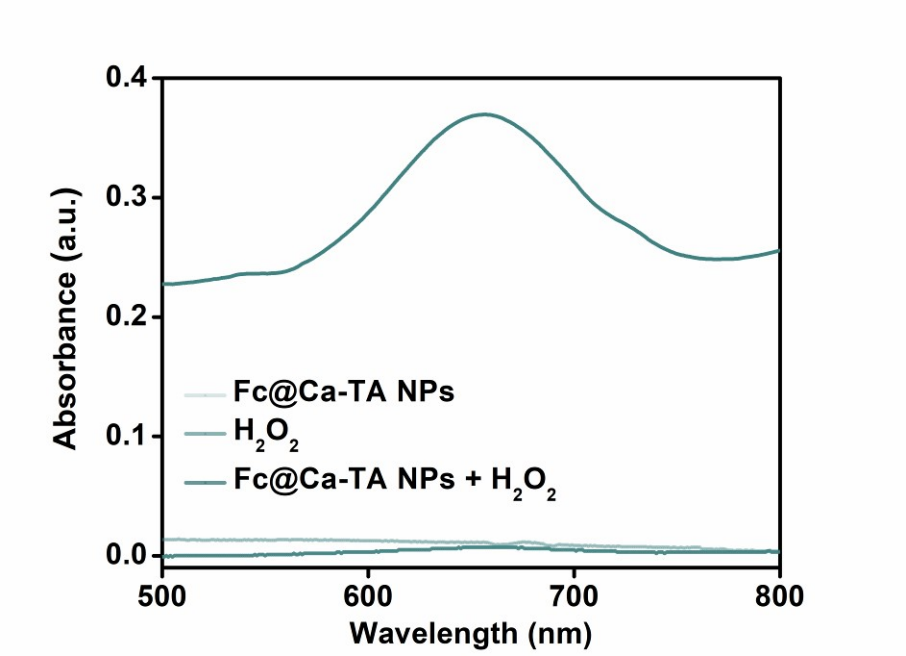

Fig. S17. Oxidation of TMB treated with Fc@Ca-TA NPs or/and H_2O_2 at pH 5.5 (Fe in Fc@Ca-TA NPs: 10 μg mL^{-1}, H_2O_2: 1 mM). There was no oxidized TMB when only Fc@Ca-TA NPs or H_2O_2 was present, revealing the occurrence of Fenton reaction between H_2O_2 and generated Fe^{2+} from Fc@Ca-TA NPs.

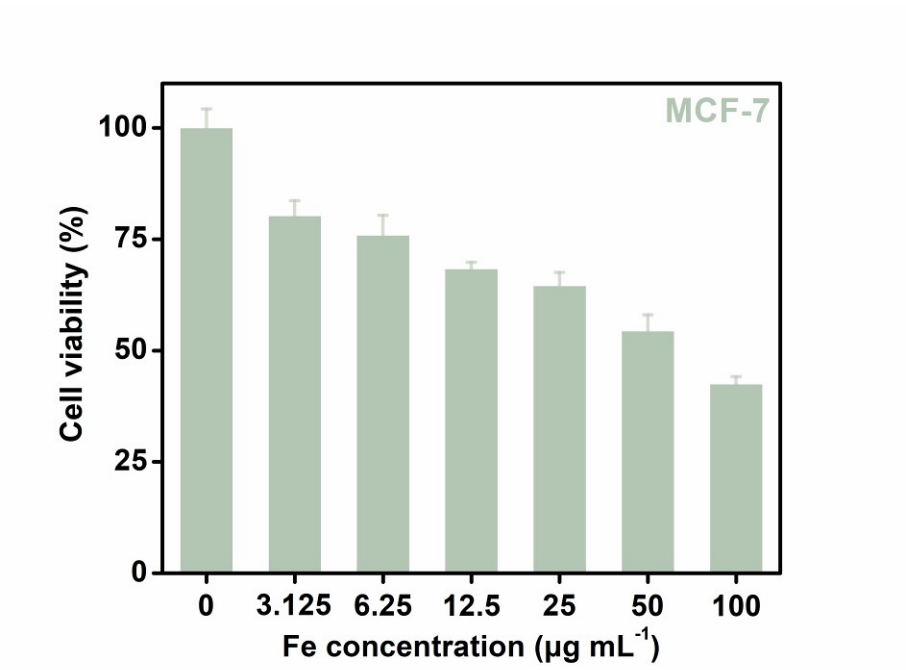

Fig. S18. Cell viability of MCF-7 cells incubated with Fc@Ca-TA NPs for 24 h. Data are presented as the mean ± SD (n = 5).

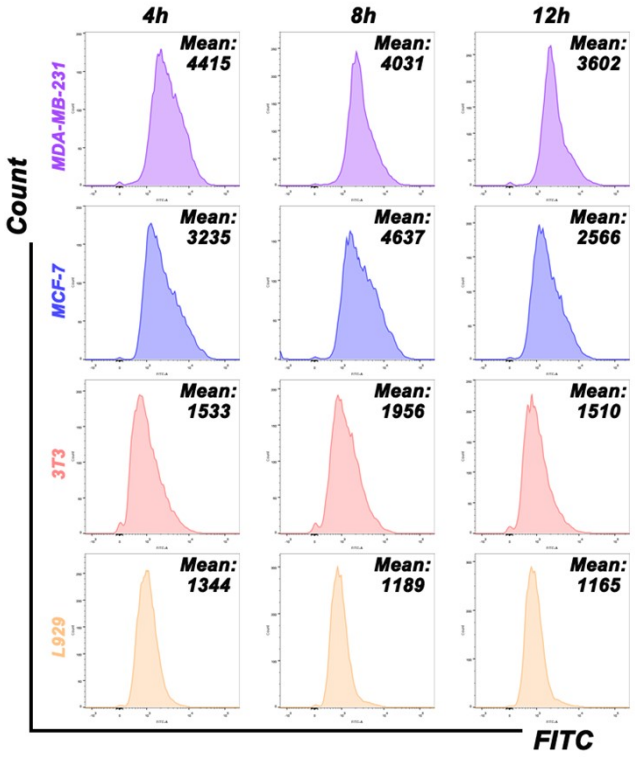

Fig. S19. Flow cytometry curves of cell lines incubated with FITC-labeled Fc@Ca-TA NPs. Whether incubated for 4h, 8h and 12h, the fluorescence intensity in MDA-MB-231 and MCF-7 cells was significantly higher than that in 3T3 and L929 cells, indicating that the tumor cells were able to take in more Fc@Ca-TA NPs.

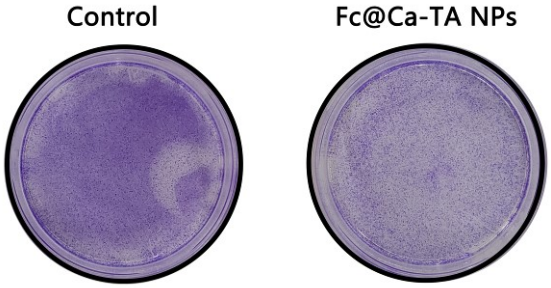

Fig. S20. Crystal violet staining of MDA-MB-231 cells incubated with Fc@Ca-TA NPs (Fe in Fc@Ca-TA NPs: 100 μg mL^{-1}) for 24 h. There were significantly reduced cell colonies after the MDA-MB-231 cells were incubated with Fc@Ca-TA NPs.

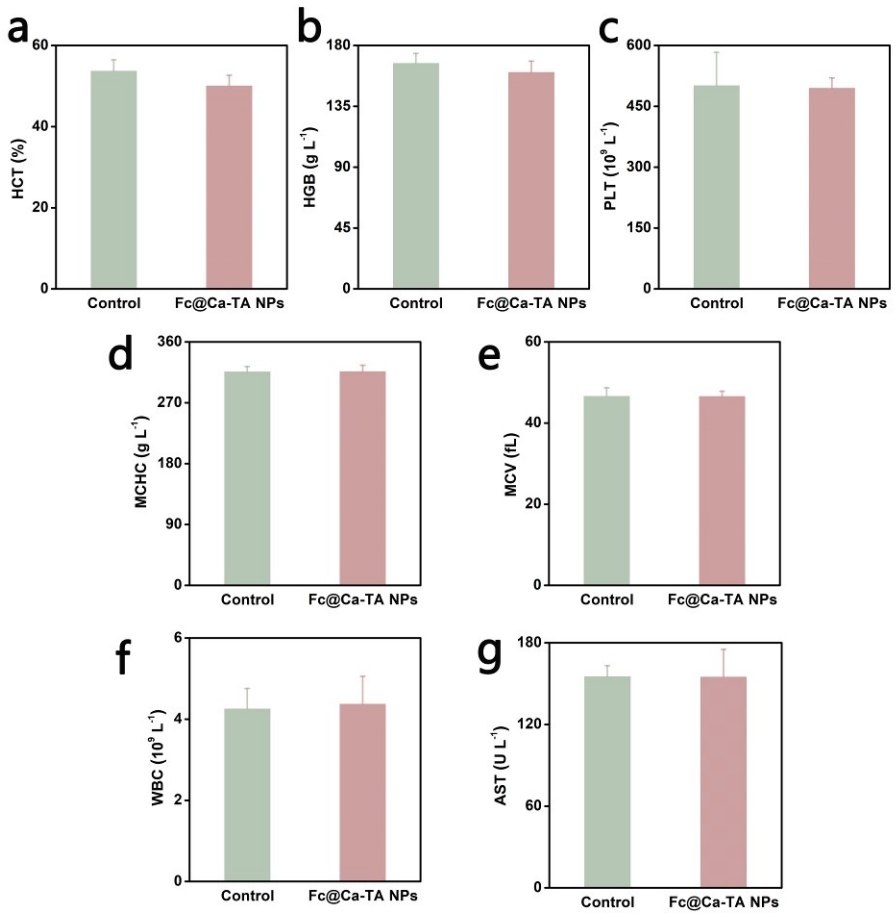

Fig. S21. (a-g) Blood biochemistry and hematology of mice intravenously injected with Fc@Ca-TA NPs (Fe: 8 mg mL^{-1}, 100 μL) or saline. Data are presented as the mean ± SD (n = 5). RBC: red blood cells; MCH: mean corpuscular hemoglobin; BUN: blood urea nitrogen; ALT: alanine aminotransferase; HCT: hematocrit; HGB: hemoglobin concentration; PLT: platelets; MCHC: mean corpuscular hemoglobin concentration; MCV: mean corpuscular volume; WBC: white blood cells; AST: aspartate aminotransferase.

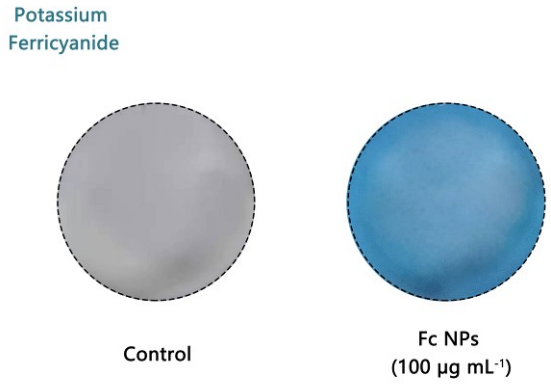

Fig. S22. Potassium ferricyanide staining of MDA-MB-231 cells incubated with Fc NPs (Fe in Fc@Ca-TA NPs: 100 μg mL^{-1}) for 12 h.

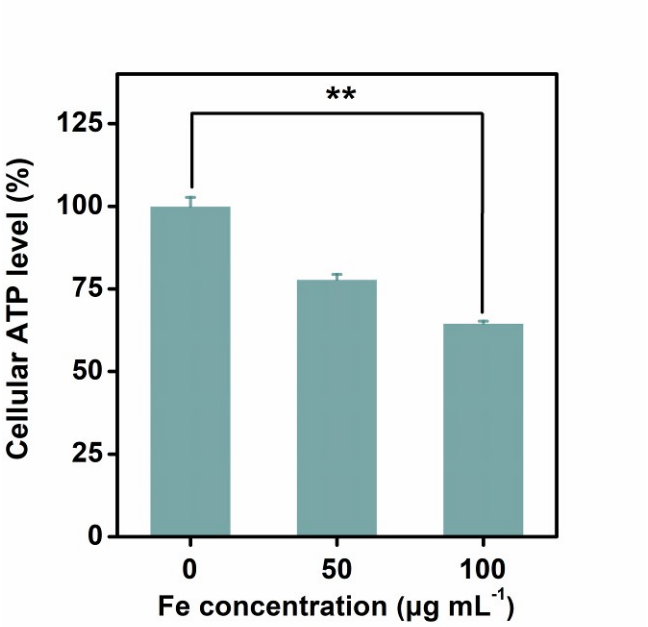

Fig. S23. Intracellular ATP levels of MDA-MB-231 cells incubated with Fc@Ca-TA NPs for 12 h. There were significantly down-regulated ATP levels after the MDA-MB-231 cells were incubated with Fc@Ca-TA NPs. Data are presented as the mean ± SD (n = 5).

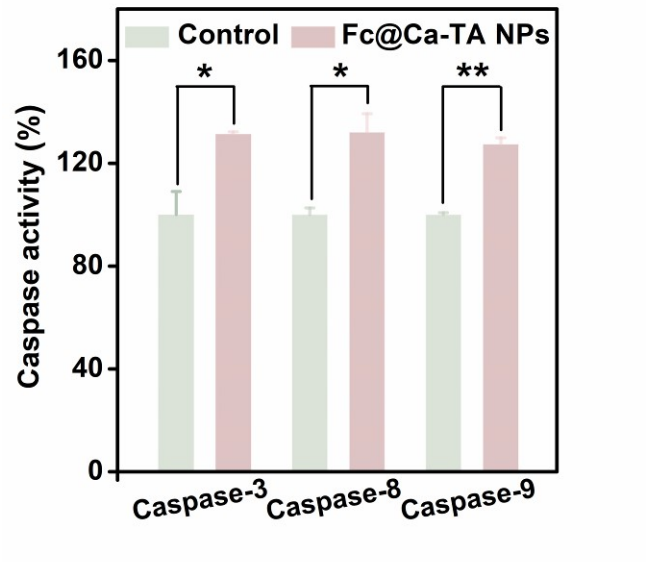

Fig. S24. Caspase activity of MDA-MB-231 cells incubated with Fc@Ca-TA NPs (Fe in Fc@Ca-TA NPs: 100 μg mL^{-1}) for 24 h. There were significantly up-regulated ATP levels after the MDA-MB-231 cells were incubated with Fc@Ca-TA NPs. Data are presented as the mean ± SD (n = 5).

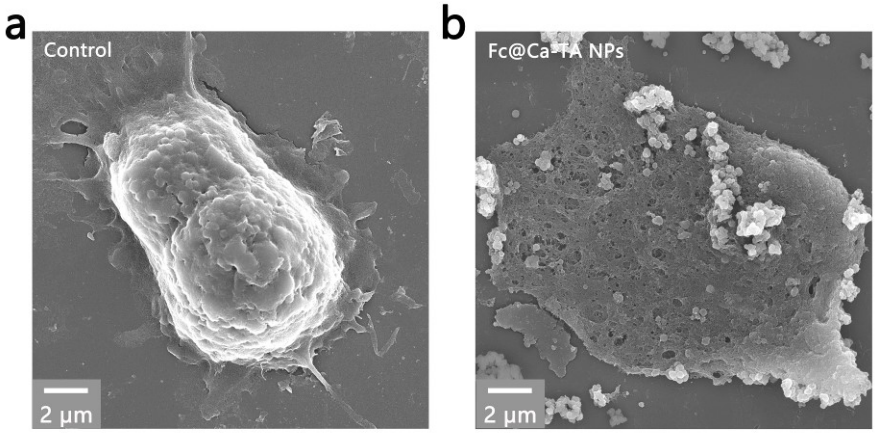

Fig. S25. (a,b) SEM image of MDA-MB-231 cells incubated without/with Fc@Ca-TA NPs (Fe in Fc@Ca-TA NPs: 100 μg mL^{-1}) for 24 h. There was a marked destruction of the cell structure of MDA-MB-231 cells incubated with Fc@Ca-TA NPs.

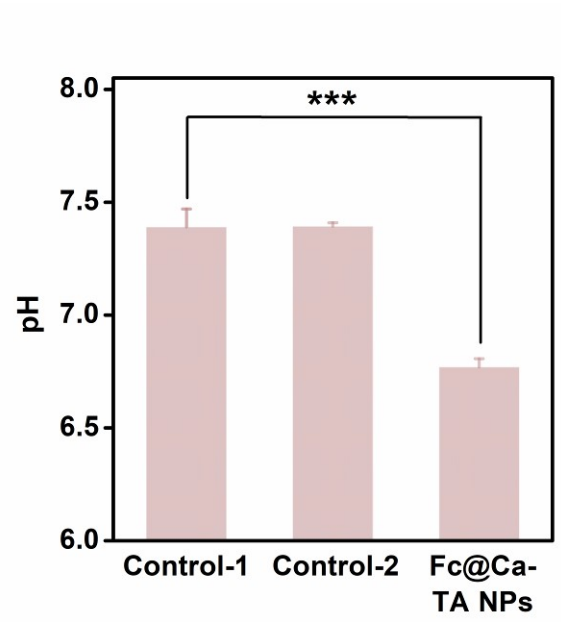

Fig. S26. pH value of DMEM after different treatments. Group Control-1: fresh DMEM; Group Control-2: DMEM after 24h co-incubation with MDA-MB-231cells; Group Fc@Ca-TA NPs: DMEM after 24h co-incubation with MDA-MB-231cells and Fc@Ca-TA NPs (Fe in Fc@Ca-TA NPs: 100 μg mL^{-1}) for 24 h. There was a marked

pH reduction in Group Fc@Ca-TA NPs. Data are presented as the mean ± SD (n = 5).

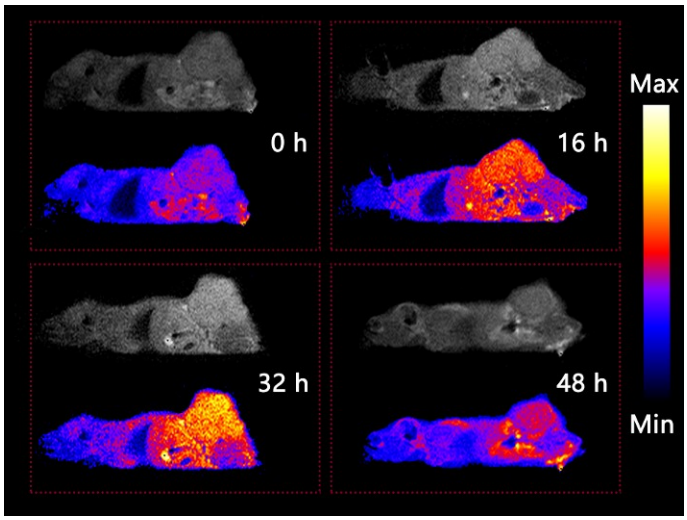

Fig. S27. MR images of mice intravenously injected with Fc@Ca-TA NPs (Fe: 4 mg mL^{-1}, 50 μL). There was a clearly enhanced T_1 signal intensity within the tumor region at 32 h post intravenous injection of Fc@Ca-TA NPs.